Theoretical design of a readout system for the Flux Qubit-Resonator Rabi Model in the ultrastrong coupling regime

Ceren Burçak Dağ
Supervisors: Dr. Pol Forn-Díaz and Assoc. Prof. Christopher Wilson

Institute for Quantum Computing
August 2014

Outline

Outline

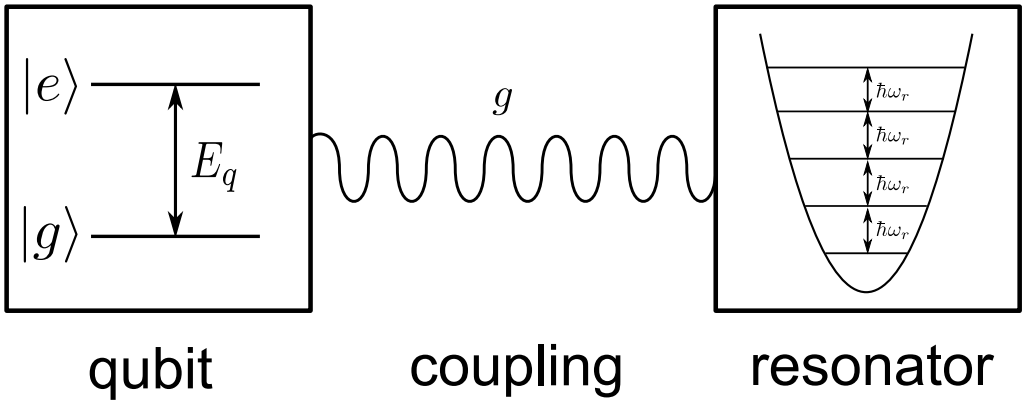

Figure : A schematic for the Rabi Model, represents an interaction between a two-level system and a quantum harmonic oscillator, (schematic copyright S. Ashhab and F. Nori).

- The main parameters of the system: ω_{qb}, ω_r and g coupling strength.
- When $g \ll \omega_{qb,r}$ and the losses dominate the coupling strength: weak coupling regime.
- When $g < \omega_{qb,r}$ but the interaction dominates the losses: strong coupling regime.
- When $g \approx \omega_{qb,r}$: ultrastrong coupling regime.
- When $g > \omega_{qb,r}$: deep strong coupling regime.

Introduction

Jaynes-Cummings Model

- The energy level structure of Rabi Model is only solvable in terms of special functions, recently [Braak2011]. So we numerically solve the Rabi Model by truncating its infinite dimensional Hilbert space.
- An analytical solution is possible for the Rabi Model in the weak coupling regime under Rotating Wave Approximation $\rightarrow$ Jaynes-Cummings Model.

Introduction

Comparison of circuit-QED with the atomic QED systems

System Type	cQED	atomic QED
Parameter variability:	changeable	fixed and identical
Scalability:	high	not at all
Decoherency:	greater	lesser

Table : The comparison of the cQED and atomic QED systems.

Introduction

QND Measurement

- Quantum Nondemolition Measurement is an indirect method to read-out the information stored in the qubit in a quantum mechanical system.
- The dispersive regime of the Jaynes-Cummings Model is utilized for QND measurement in the cQED experiments.
- This research proposes a possible QND measurement method for the Rabi Model in the ultrastrong coupling regime.

Outline

Constructing the Rabi Hamiltonian

The Quantization of the LC Resonator

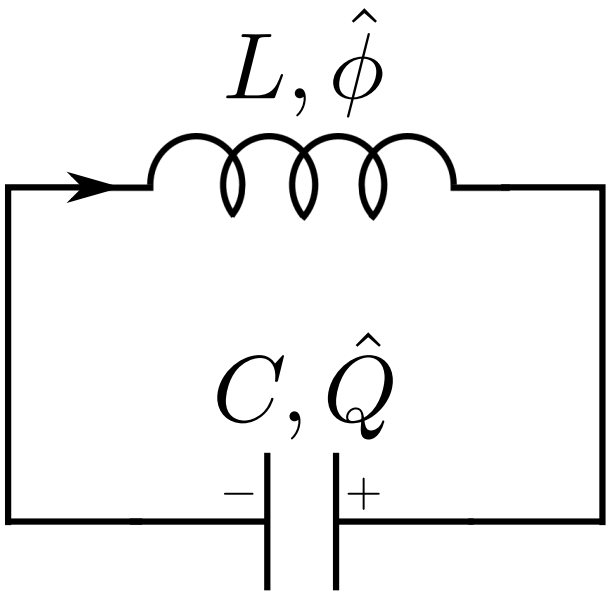

Figure : Schematic of an LC resonator, shown with its quantized canonical variables.

Classically:

$$H = \frac{Q^2}{2C} + \frac{\phi^2}{2L} \tag{1}$$

By using Hamilton's equations one can obtain the well-known harmonic oscillator differential equation whose solution is,

$$Q(t) = C_1 \sin(\omega t) + C_2 \cos(\omega t) \tag{2}$$

where $\omega = 1/\sqrt{LC}$ and C_1, C_2 are some arbitrary real constants to be determined by the initial conditions. In order to quantize the LC oscillator, let us rewrite it

$$\begin{aligned} H &= \frac{1}{2L}\left(\left(\sqrt{\frac{L}{C}}Q\right)^2 + \phi^2\right) \\ &= \frac{1}{2L}\left(\sqrt{\frac{L}{C}}Q - i\phi\right)\left(\sqrt{\frac{L}{C}}Q + i\phi\right) \end{aligned} \tag{3}$$

The canonical quantization dictates the exchange of the dynamical variables by the operators with a commutation relation. Then the Hamiltonian will be,

$$\hat{H} = \frac{\hat{Q}^2}{2C} + \frac{\hat{\phi}^2}{2L}. \tag{4}$$

where the commutation relation is $\left[\hat{\phi}, \hat{Q}\right] = i\hbar$. By applying the same procedure to the factorized parts,

$$\hat{a} = \sqrt{\frac{1}{2L}}\left(\sqrt{\frac{L}{C}}\hat{Q} + i\hat{\phi}\right), \tag{5}$$

$$\hat{a}^\dagger = \sqrt{\frac{1}{2L}}\left(\sqrt{\frac{L}{C}}\hat{Q} - i\hat{\phi}\right). \tag{6}$$

Then finding $\hat{a}^\dagger \hat{a}$,

$$\hat{a}^\dagger \hat{a} = \frac{\hat{Q}^2}{2C} + \frac{\hat{\phi}^2}{2L} - i\frac{1}{2\sqrt{LC}}\left[\hat{Q}, \hat{\phi}\right], \tag{7}$$

and by exploiting the commutation relation and substituting $\omega_{LC} = 1/\sqrt{LC}$, the Hamiltonian will be,

$$\hat{H} = \hbar\omega\left(\hat{a}^\dagger \hat{a} + \frac{1}{2}\right) = \hbar\omega\left(\hat{n} + \frac{1}{2}\right). \tag{8}$$

Then the field operators in terms of annihilation and creation operators,

$$\hat{Q} = \left(\frac{\hbar}{2}\right)^{1/2} \left(\frac{C}{L}\right)^{1/4} (\hat{a} + \hat{a}^\dagger), \tag{9}$$

$$\hat{\phi} = -i \left(\frac{\hbar}{2}\right)^{1/2} \left(\frac{L}{C}\right)^{1/4} (\hat{a} - \hat{a}^\dagger). \tag{10}$$

just like the electric and magnetic fields in the quantization of the EM field. We define $\sqrt{L/C} = Z_0$, which is introduced as the impedance also used in classical microwave theory.

Constructing the Rabi Hamiltonian

Josephson junction

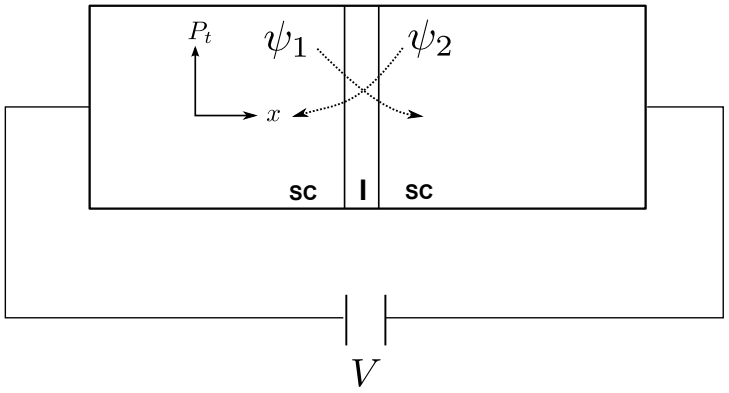

$$I = I_o \sin\delta, \tag{11}$$

$$\frac{d\delta}{dt} = \frac{2e}{\hbar} V. \tag{12}$$

where δ is the phase change between the two ends of the element and I_0 is the critical current, which is the maximum amount of current that can flow through a superconducting junction.

Constructing the Rabi Hamiltonian

Flux qubit

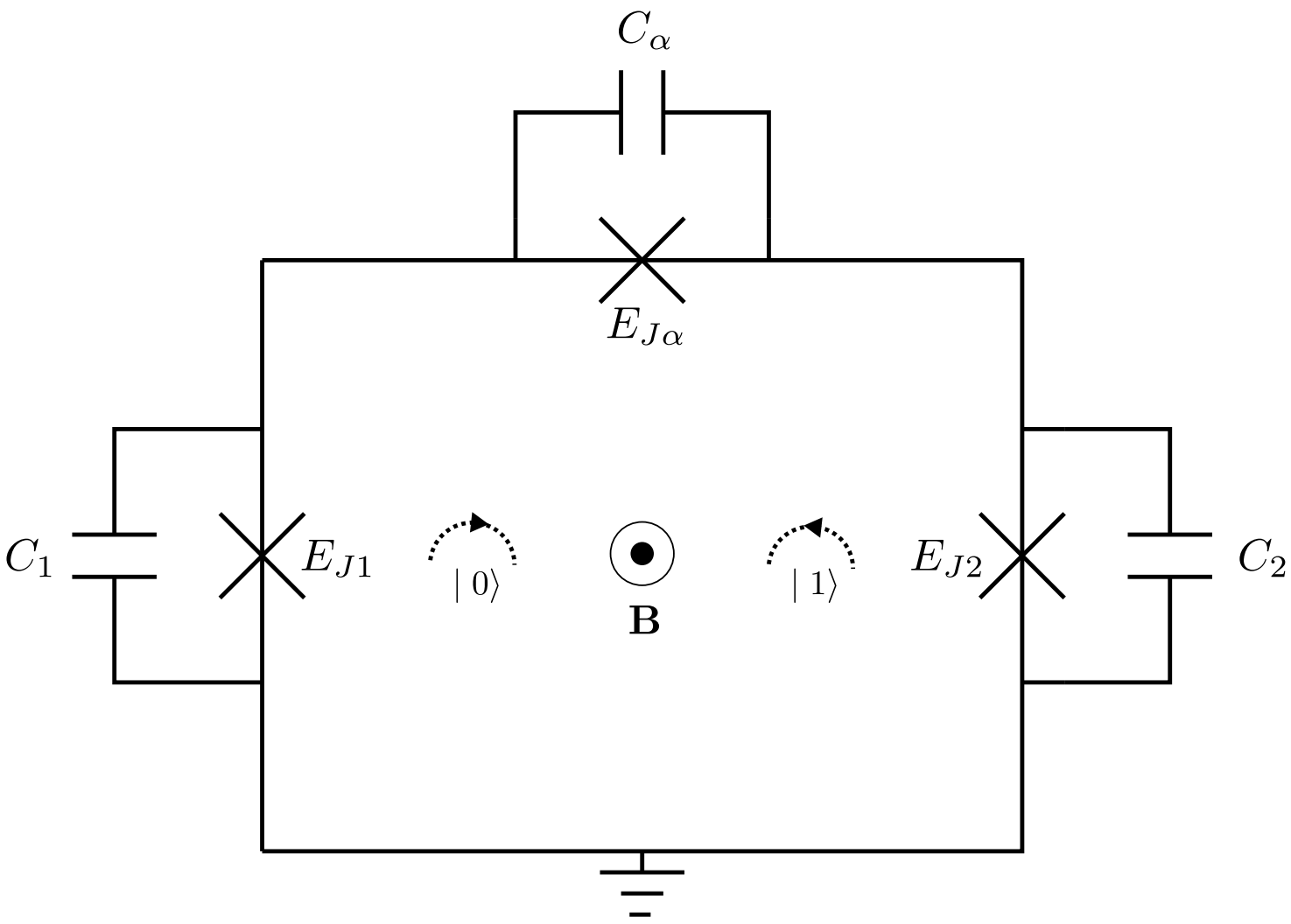

The energy of a single Josephson junction,

$$E = \int_0^t IVd\tau = \int_0^t I_o \frac{2e}{\hbar} \sin\delta \frac{d\delta}{d\tau} d\tau = I_o \frac{2e}{\hbar} \int_0^\delta \sin\delta' d\delta' = E_J(1-\cos\delta). \tag{13}$$

The wave functions must be single valued along a closed path, which motivates the flux quantization condition:

$$\phi_1 - \phi_2 + \phi_\alpha + 2\pi f = 0. \tag{14}$$

where f is the magnetic frustration and is defined as $f = \frac{\Phi}{\Phi_0}$, Φ is the externally applied magnetic flux and $\Phi_0 = h/2e$ is the flux quantum. Then the energy of the flux qubit,

$$\begin{aligned} U &= E_J(1 - \cos\delta_1 + 1 - \cos\delta_2 + \alpha - \alpha\cos\delta_\alpha) \\ &= E_J(2 + \alpha - \cos\delta_1 - \cos\delta_2 - \alpha\cos(2\pi f + \delta_1 - \delta_2)), \end{aligned} \tag{15}$$

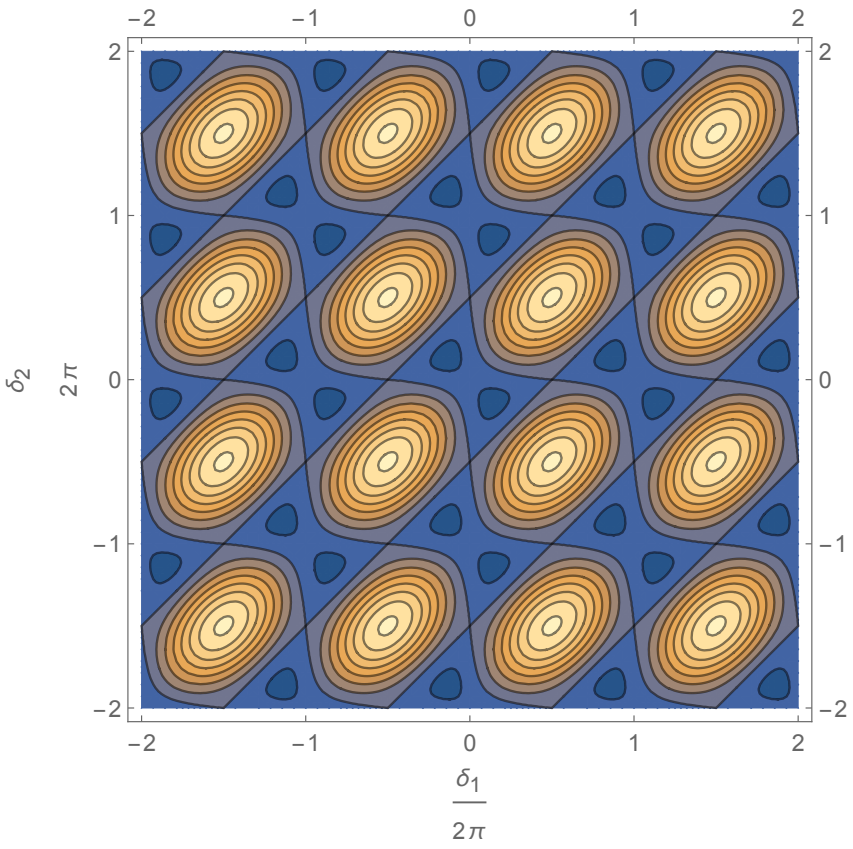

Figure : The contour plot for the energy of the flux qubit with respect to its two different phases when $\alpha = 0.8$ at symmetry point, $f = 0.5$.

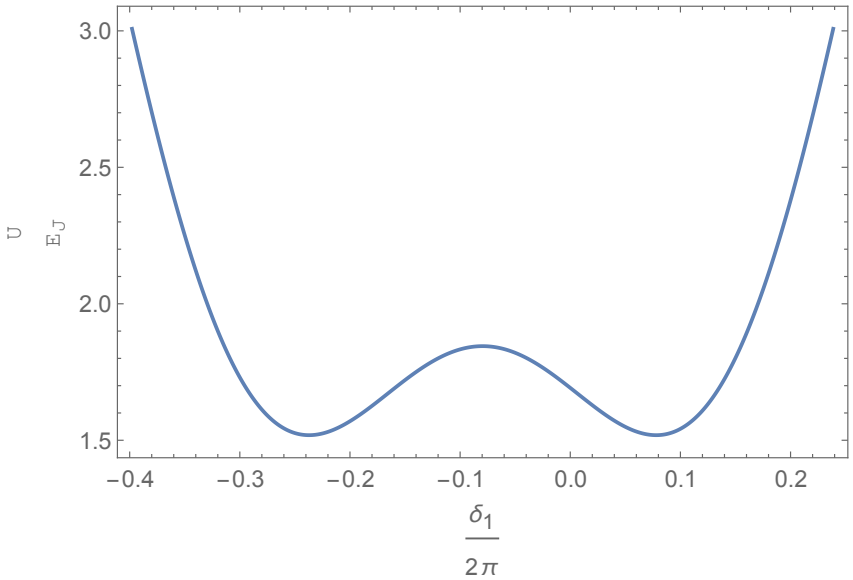

Figure : Two dips seen in the energy plot of the flux qubit which corresponds to two stable solutions.

These stable configurations represent the circulating DC currents of opposite direction through the circuit. These currents are called *persistent currents*, [Mooij1999].

Constructing the Rabi Hamiltonian

The Hamiltonian of the Flux Qubit

$$H = \frac{\hbar\Delta}{2}\sigma_x + \frac{\epsilon}{2}\sigma_z, \tag{16}$$

where $\epsilon = 2I_p\Phi_o\left(f - \frac{1}{2}\right)$ is the magnetic energy of the flux qubit and Δ is the tunnelling rate of the wave functions in the potential energy created by three Josephson junctions in a flux qubit and I_p is the persistent current in the flux qubit.

Diagonalized Hamiltonian:

$$\Lambda = \begin{pmatrix} -\frac{1}{2}\sqrt{\epsilon^2 + \Delta^2\hbar^2} & 0 \\ 0 & \frac{1}{2}\sqrt{\epsilon^2 + \Delta^2\hbar^2} \end{pmatrix}, \tag{17}$$

when the eigenvectors are chosen as,

$$\phi_1 = (\cos\theta/2, \sin\theta/2)\,, \tag{18}$$

$$\phi_2 = (-\sin\theta/2, \cos\theta/2)\,, \tag{19}$$

where $\tan\theta = \hbar\Delta/\epsilon$, so that the transformation matrix is

$$T = \begin{pmatrix} \cos\theta/2 & -\sin\theta/2 \\ \sin\theta/2 & \cos\theta/2 \end{pmatrix}. \tag{20}$$

Constructing the Rabi Hamiltonian

Rabi Hamiltonian will be in general composed of three parts:

$$\hat{H} = \hat{H}_{qb} + \hat{H}_r + \hat{H}_I. \tag{21}$$

The Hamiltonian for the flux qubit explicitly,

$$\hat{H}_{qb} = \mp\frac{1}{2}\sqrt{4\left(f - \frac{1}{2}\right)^2 I_p^2\Phi_0^2 + \Delta^2\hbar^2} \equiv \mp\frac{\hbar\omega_{qb}}{2}, \tag{22}$$

The Hamiltonian for the LC resonator,

$$\hat{H}_r = \hbar\omega_r\left(\hat{a}^\dagger\hat{a} + \frac{1}{2}\right). \tag{23}$$

Finally the interaction term through electric dipole coupling in general,

$$\hat{H}_I = -\hat{\mathbf{d}} \cdot \hat{\mathbf{E}}, \tag{24}$$

where $\hat{\mathbf{d}}$ is a dipole operator which consists of atomic transition operators. Let us introduce atomic transition operators in a two-level system, which enable the transitions from ground to excited state (or vice versa):

$$\hat{\sigma}_+ \equiv |e\rangle \langle g| , \qquad \hat{\sigma}_- \equiv |g\rangle \langle e| . \tag{25}$$

By recalling the form of the quantized charge in the Quantum LC Resonator, the interaction term can be expressed as,

$$\hat{H}_I = \hbar g(\hat{\sigma}_+ + \hat{\sigma}_-)(\hat{a} + \hat{a}^\dagger) = \hbar g \sigma_x(\hat{a} + \hat{a}^\dagger). \tag{26}$$

By taking the fact that the coupling is through the interaction of the magnetic field of the resonator and the magnetic moment of the qubit into account, the Rabi Hamiltonian for the flux qubit-LC resonator system,

$$H = \frac{\hbar\Delta}{2}\sigma_x + I_p\Phi_o\left(f - \frac{1}{2}\right)\sigma_z + \hbar g\sigma_z(\hat{a} + \hat{a}^\dagger) + \hbar\omega_r\left(\hat{a}^\dagger\hat{a} + \frac{1}{2}\right). \tag{27}$$

In order to bring it to the known form of cQED Hamiltonian, we will use the diagonalized form of the qubit Hamiltonian and express the other terms in the eigenbasis of the qubit Hamiltonian.

So we obtain the total Hamiltonian as

$$\hat{H} = \frac{\hbar\omega_{qb}}{2}\sigma_z - \hbar g \sin\theta \sigma_x(\hat{a}^\dagger + \hat{a}) + \hbar\omega_r \left(\hat{a}^\dagger \hat{a} + \frac{1}{2}\right), \qquad (28)$$

where $\frac{\Delta}{\omega_{qb}} \equiv \sin\theta$ and (recalling)
$\frac{\hbar\omega_{qb}}{2} = \mp\frac{1}{2}\sqrt{4\left(f - \frac{1}{2}\right)^2 I_p^2 \Phi_0^2 + \Delta^2\hbar^2}$.

Constructing the Rabi Hamiltonian

Rotating Wave Approximation

Interaction terms:

$$\hat{\sigma}_+ \hat{a} \propto e^{i(\omega_{qb}-\omega_r)t} \tag{29}$$

$$\hat{\sigma}_- \hat{a} \propto e^{-i(\omega_{qb}+\omega_r)t} \tag{30}$$

$$\hat{\sigma}_+ \hat{a}^\dagger \propto e^{i(\omega_{qb}+\omega_r)t} \tag{31}$$

$$\hat{\sigma}_- \hat{a}^\dagger \propto e^{-i(\omega_{qb}-\omega_r)t} \tag{32}$$

Equations (30) and (31) represent fast rotating terms and also non-resonant terms in the rotating frame, so that we can apply the so-called rotating wave approximation (RWA) where we drop the fast rotating terms from the Rabi Hamiltonian. RWA is only possible under the condition:

$$\frac{g}{\omega_{qb,r}} \ll 1. \tag{33}$$

Constructing the Rabi Hamiltonian

Jaynes-Cummings Hamiltonian of Flux Qubit-LC Resonator

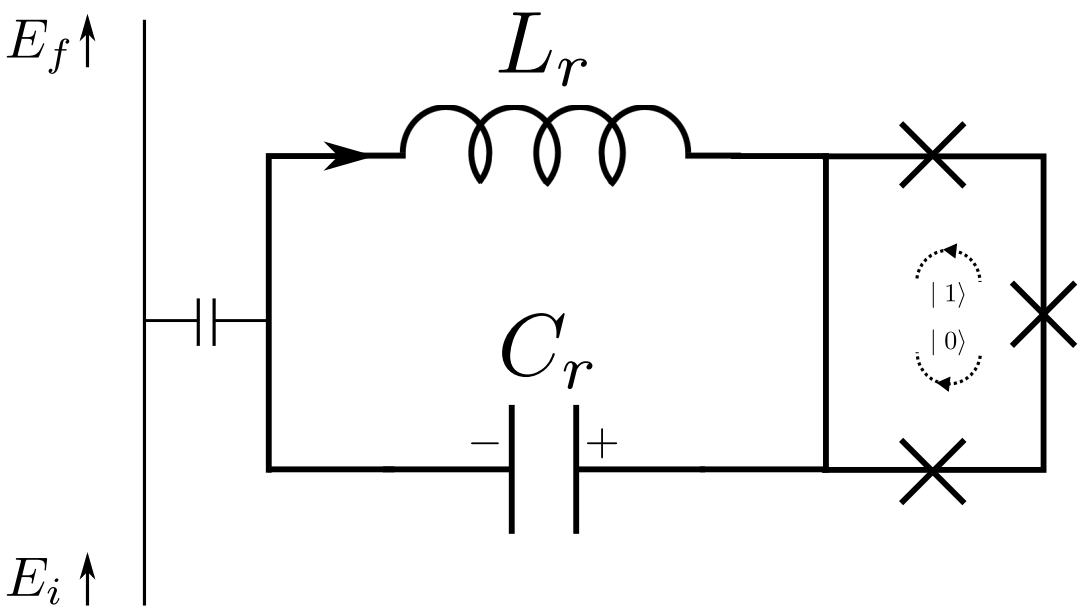

Figure : A circuit schematic which shows the JC model of a flux qubit coupled to an LC resonator.

Assuming that $\frac{g}{\omega_r} \ll 1$, the RWA can be applied to the coupling term. Then Jaynes-Cummings Hamiltonian is:

$$\hat{H} = \frac{\hbar\omega_{qb}}{2}\sigma_z - \hbar g \sin\theta \left(\hat{\sigma}_- \hat{a}^\dagger + \hat{\sigma}_+ \hat{a}\right) + \hbar\omega_r \left(\hat{a}^\dagger \hat{a} + \frac{1}{2}\right), \quad (34)$$

Now we need to construct the JC Hamiltonian matrix in order to extract the eigenenergies of the Rabi system when $\frac{g}{\omega_r} \ll 1$.

$$\hat{H} = \begin{pmatrix} \ddots & & & \\ & \frac{\hbar\omega_{qb}}{2} + \Omega_r(n) & -\hbar g \sin\theta\sqrt{n+1} & \\ & -\hbar g \sin\theta\sqrt{n+1} & -\frac{\hbar\omega_{qb}}{2} + \Omega_r(n+1) & \\ & & & \ddots \end{pmatrix}. \quad (35)$$

where $\Omega_r(n) = \hbar\omega_r\left(n + \frac{1}{2}\right)$. If we diagonalize this matrix, we will obtain different eigenvalues in the general form,

$$E_{\pm,n} = (n+1)\hbar\omega_r \pm \frac{1}{2}\sqrt{(n+1)\left(\frac{2\hbar g\Delta}{\omega_{qb}}\right)^2 + \hbar^2(\omega_{qb} - \omega_r)^2}, \quad (36)$$

where n is the excitation number. The eigenstates of JC Model are also called *the dressed states* of the JC Model.

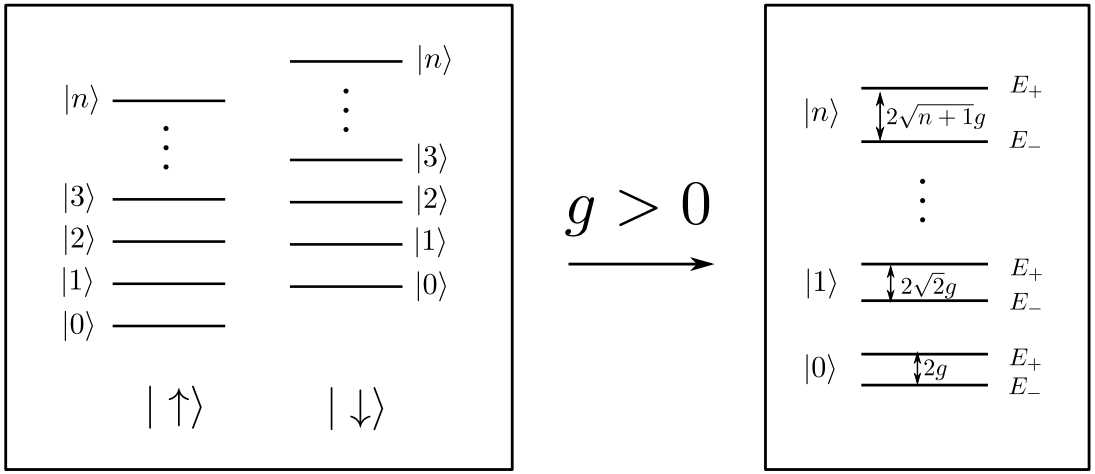

Figure : A schematic which shows the uncoupled Jaynes-Cummings states when $g = 0$ and dressed states when $g > 0$.

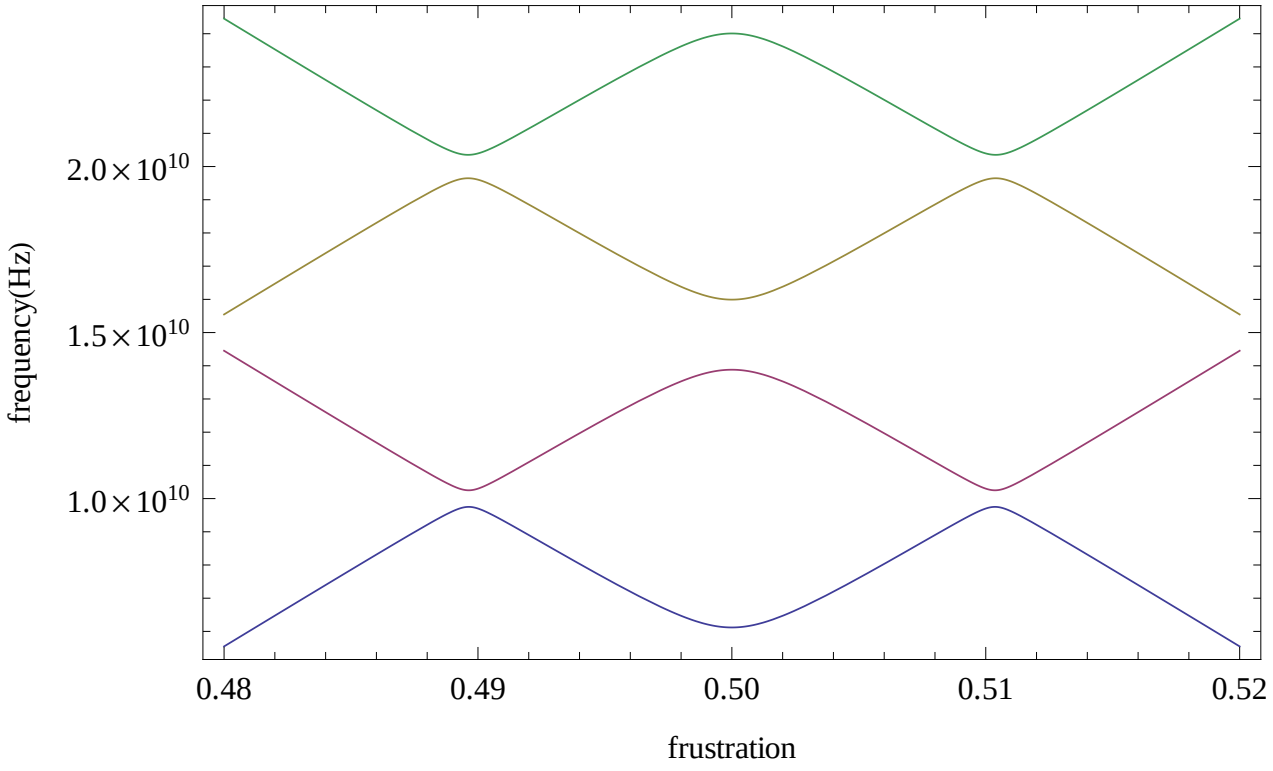

Figure : Energy levels with respect to magnetic field frustration in the qubit when up to states with two photons exist in the resonator with $g = 0.05\omega_r$, vertical axis is frequency in Hz. Pink: $E_{0,-}$, blue: $E_{0,+}$, green: $E_{1,-}$ and brown: $E_{1,+}$.

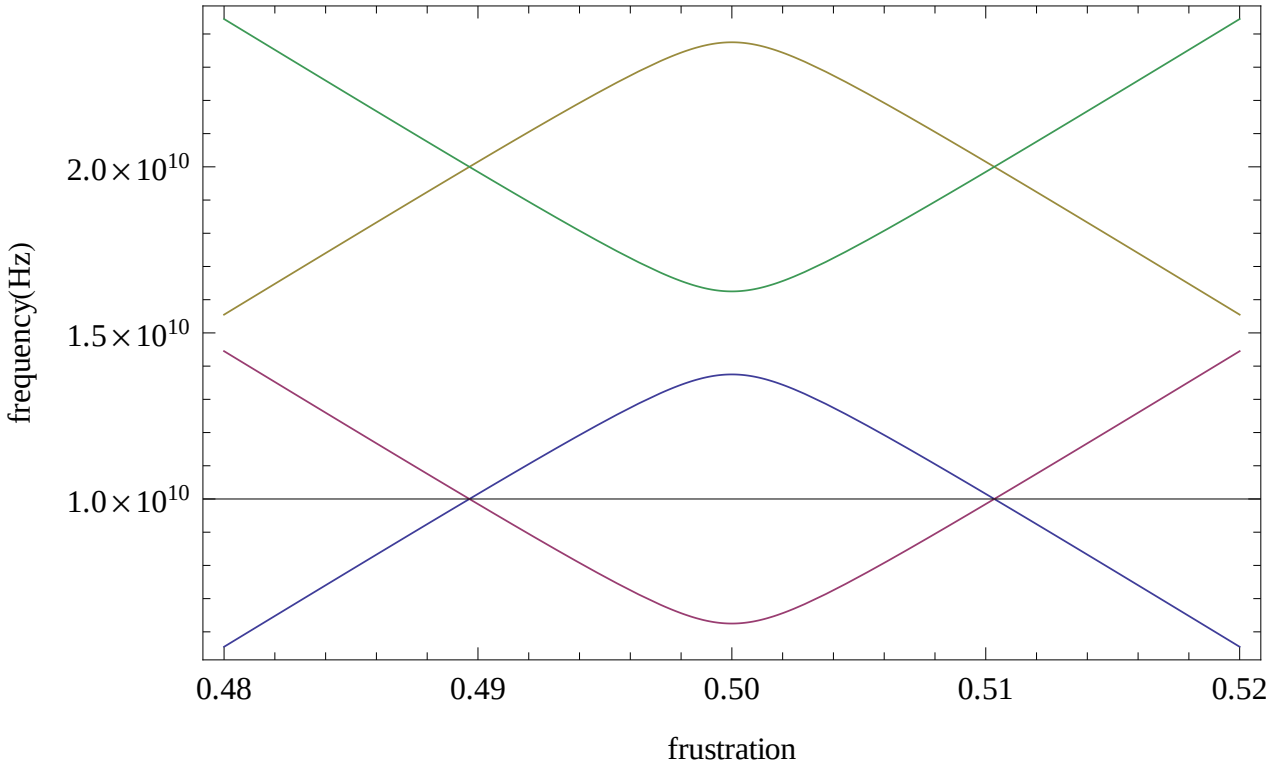

Figure : The energy levels with respect to magnetic frustration when two photons exist in the resonator with $g = 0$, vertical axis is frequency in Hz. Pink: $E_{0,-}$, blue: $E_{0,+}$, green: $E_{1,-}$ and brown: $E_{1,+}$.

Outline

Results of the Rabi Model of Flux Qubit-LC Resonator system

Parity Chains

A JC dublet:

$$|e0\rangle \leftrightarrow |g1\rangle \tag{37}$$

Rabi parity chains:

$$|g0\rangle \leftrightarrow |e1\rangle \leftrightarrow |g2\rangle \leftrightarrow |e3\rangle \leftrightarrow \ldots \quad (p = 1), \tag{38}$$

$$|e0\rangle \leftrightarrow |g1\rangle \leftrightarrow |e2\rangle \leftrightarrow |g3\rangle \leftrightarrow \ldots \quad (p = -1). \tag{39}$$

Results of the Rabi Model of Flux Qubit-LC Resonator system

Numerical Solution of Rabi Model

$$\hat{H} = \frac{\hbar\Delta}{2}(\sigma_x \otimes \mathbb{I}_n) + I_p\Phi_o\left(f - \frac{1}{2}\right)(\sigma_z \otimes \mathbb{I}_n) + \hbar g(\sigma_z \otimes (\hat{a} + \hat{a}^\dagger)) + \hbar\omega_r\left(\mathbb{I}_{qb} \otimes \left(\hat{a}^\dagger\hat{a} + \frac{1}{2}\right)\right). \tag{40}$$

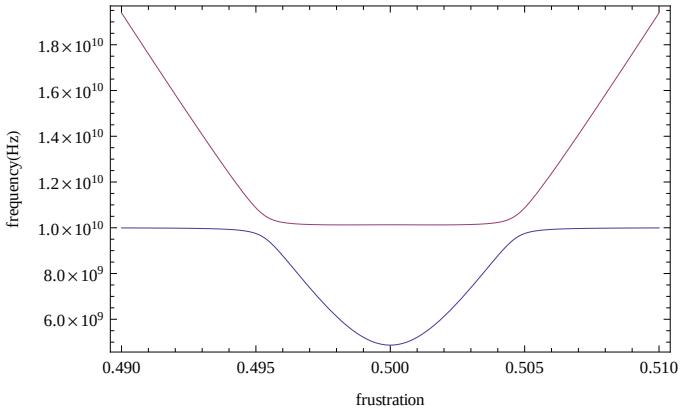

Figure : The difference between energy levels of QRM with respect to magnetic field frustration in the qubit with $g = \omega_r$.

Energy spectrum:

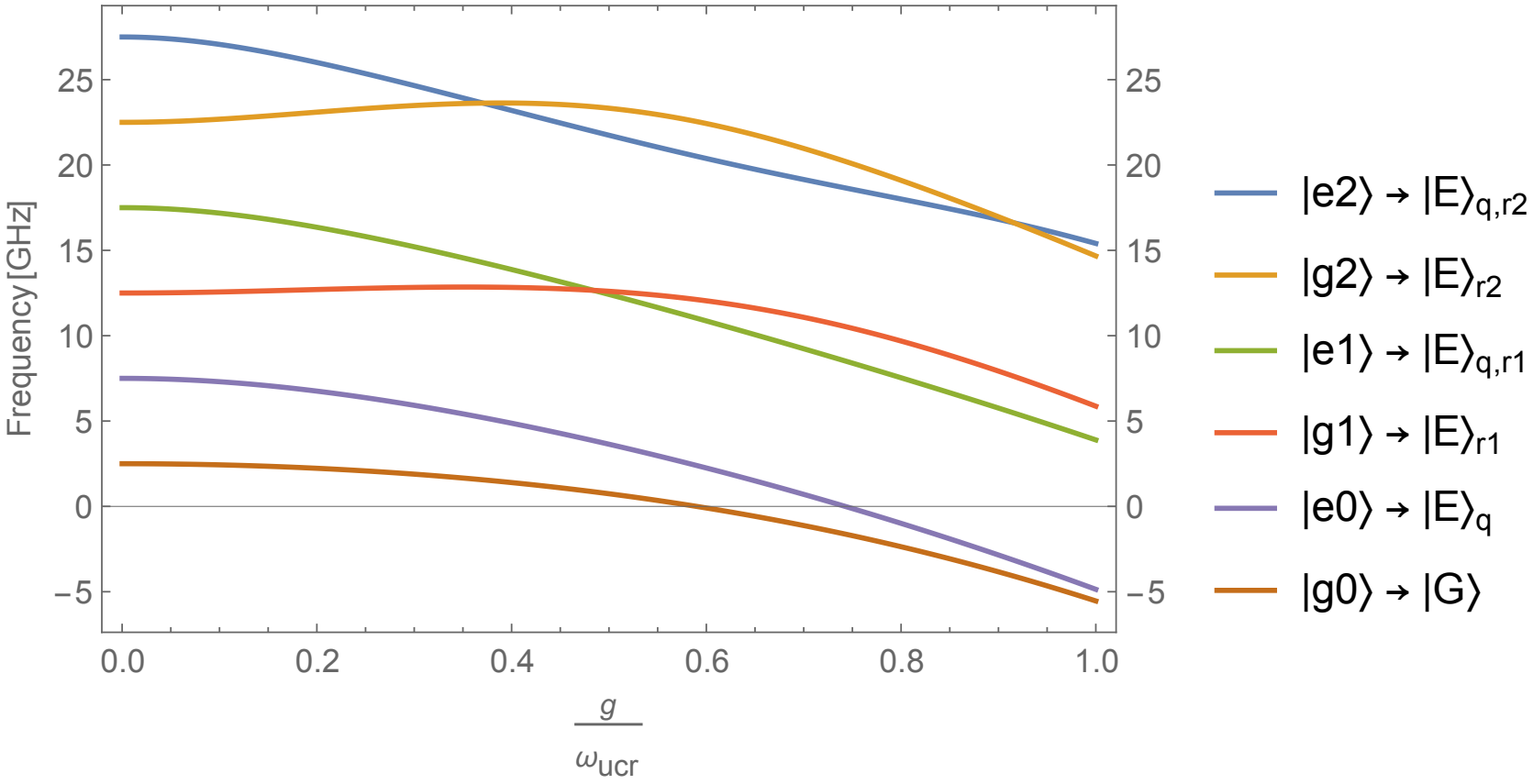

Figure : Energy levels of the quantum Rabi model with respect to g/ω_r using up to 11 Fock states in the resonator, at the symmetry point, $f = 0.5$ and $\omega_{qb} = 0.5\omega_r$.

Outline

The theoretical design of a QND measurement system for Rabi Model of Flux Qubit-Resonator

Proposed Model

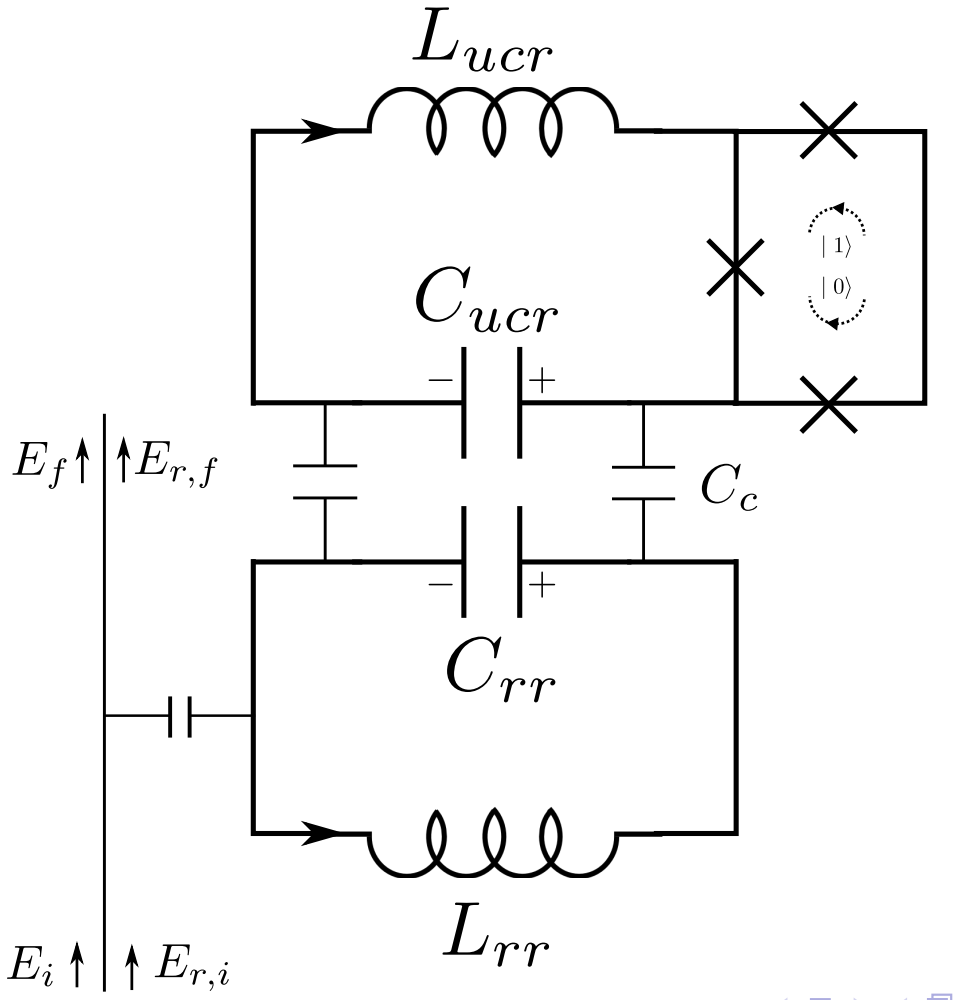

In order to understand why we proposed this model, let us investigate the dispersive regime of Jaynes-Cummings Model. The detuning is defined as $\delta = \omega_{qb} - \omega_r$. When there is a large detuning, $2g\sqrt{n+1}/\delta \ll 1$, we can expand the eigenenergies of JC Model as

$$E_{\pm}^{d} = \hbar(n+1)\left(\omega_r \pm \frac{g^2}{\delta}\frac{\Delta^2}{\omega_{qb}^2}\right) \pm \frac{\delta\hbar}{2}. \tag{41}$$

The shift $\pm\frac{g^2}{\delta}\frac{\Delta^2}{\omega_{qb}^2}$ is called Stark shift.

We can obtain more insight about the energy shifts with a Schrieffer-Wolf transformation U of the generator $S = -i\frac{g}{\delta}(a\sigma_+ - a^\dagger\sigma_-)$,

$$H_{eff} = UHU^{-1} = e^{iS}He^{-iS} = H + i[S,H] + \frac{i^2}{2}[S,[S,H]] + \ldots \quad (42)$$

Apply it to the JC Hamiltonian and expanding to second order in g/δ leads to,

$$H_{JC}^d \approx \hbar\left(\omega_r + \frac{g^2}{\delta}\sin^2\theta\sigma_z\right)a^\dagger a + \frac{\hbar}{2}\left(\omega_{qb} + \frac{g^2}{\delta}\sin^2\theta\right)\sigma_z. \quad (43)$$

Hamiltonian:

$$\hat{H} = \frac{\hbar\Delta}{2}\sigma_x + I_p\Phi_o\left(f - \frac{1}{2}\right)\sigma_z + \hbar g\sigma_z(\hat{a} + \hat{a}^\dagger) + \hbar\omega_{UCR}\left(\hat{a}^\dagger\hat{a} + \frac{1}{2}\right) + \hbar\omega_{RR}\left(\hat{b}^\dagger\hat{b} + \frac{1}{2}\right) - \hbar g_r\left(\hat{a}^\dagger + \hat{a}\right)\left(\hat{b}^\dagger + \hat{b}\right), \tag{44}$$

$\hat{a}$: annihilation operator of UCR, $\hat{b}$: annihilation operator of RR, $g_r = \frac{\omega_c^2\hbar}{2\sqrt{\omega_{UCR}\omega_{RR}}}$.

- The first set of parameters is $\Delta/2\pi = 5$ GHz, $\omega_{UCR}/2\pi = 10$ GHz, $\omega_{RR}/2\pi = 9$ GHz, $\omega_c/2\pi = 1$ GHz so that the total coupling between the resonators is $g_r = 52.7$ MHz.
- The second set of parameters is $\Delta/2\pi = 12$ GHz, $\omega_{UCR}/2\pi = 10$ GHz, $\omega_{RR}/2\pi = 9$ GHz and $\omega_c/2\pi = 1$ GHz.
- The third set of parameters is $\Delta/2\pi = 9.5$ GHz, $\omega_{UCR}/2\pi = 10$ GHz, $\omega_{RR}/2\pi = 9$ GHz and $\omega_c/2\pi = 1$ GHz.

The theoretical design of a QND measurement system for Rabi Model of Flux Qubit-Resonator

Results

Detuning (between UCR and qubit): 5 GHz. We will show:

- The compositions of the lowest four states with respect to the coupling strengths $\rightarrow |\phi\rangle = \sum_i c_i |\psi_i\rangle$.
- The amount of the entanglement between RR and the rest of the system.
- If RR is sufficiently disentagled from rest of the system, energy level structure and the energy shifts observed in the RR's frequency.

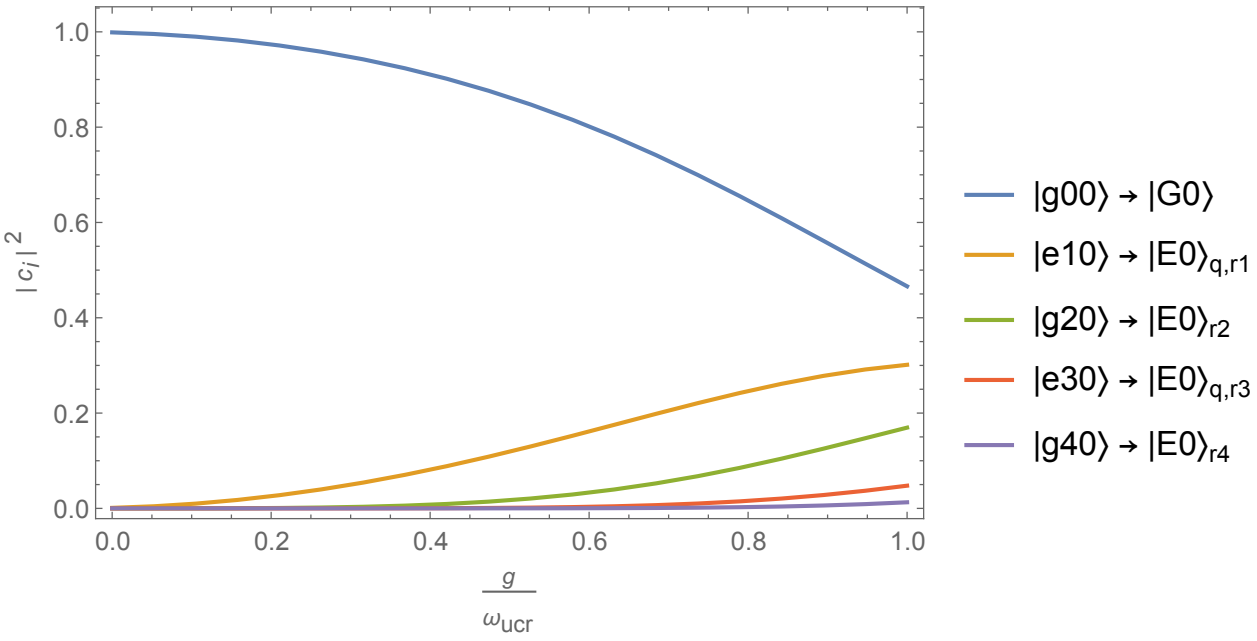

Figure : The decomposition of the state $|G0\rangle$ to the other states with respect to g coupling.

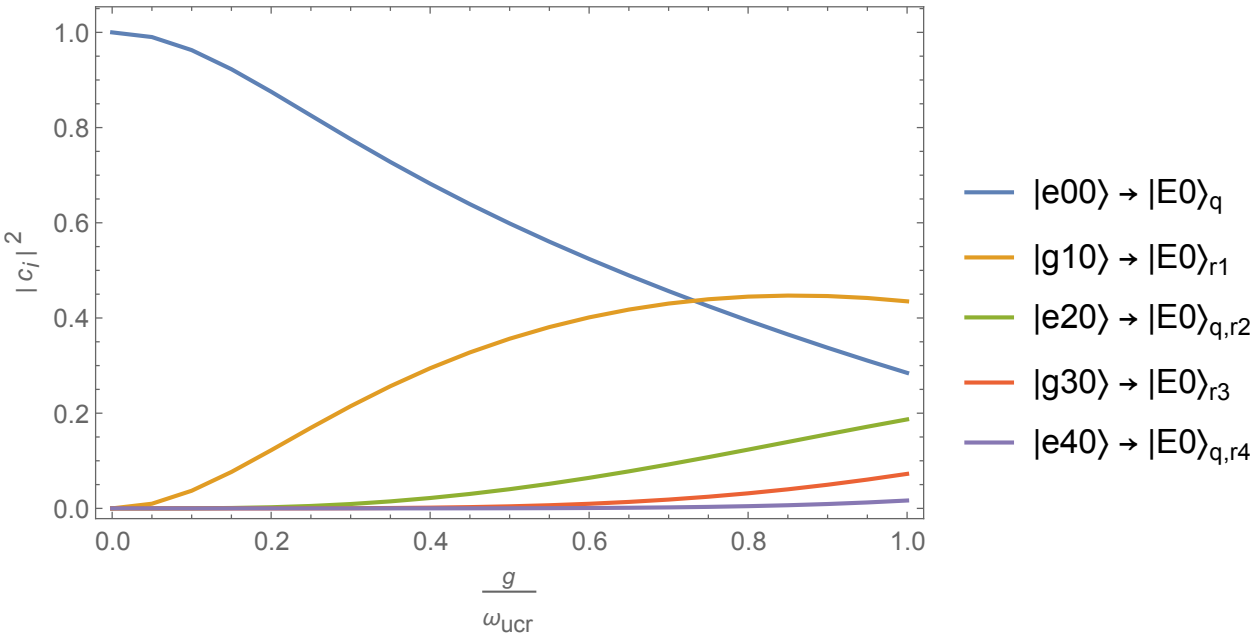

Figure : The decomposition of the state $|E0\rangle_q$ to the other states with respect to g coupling.

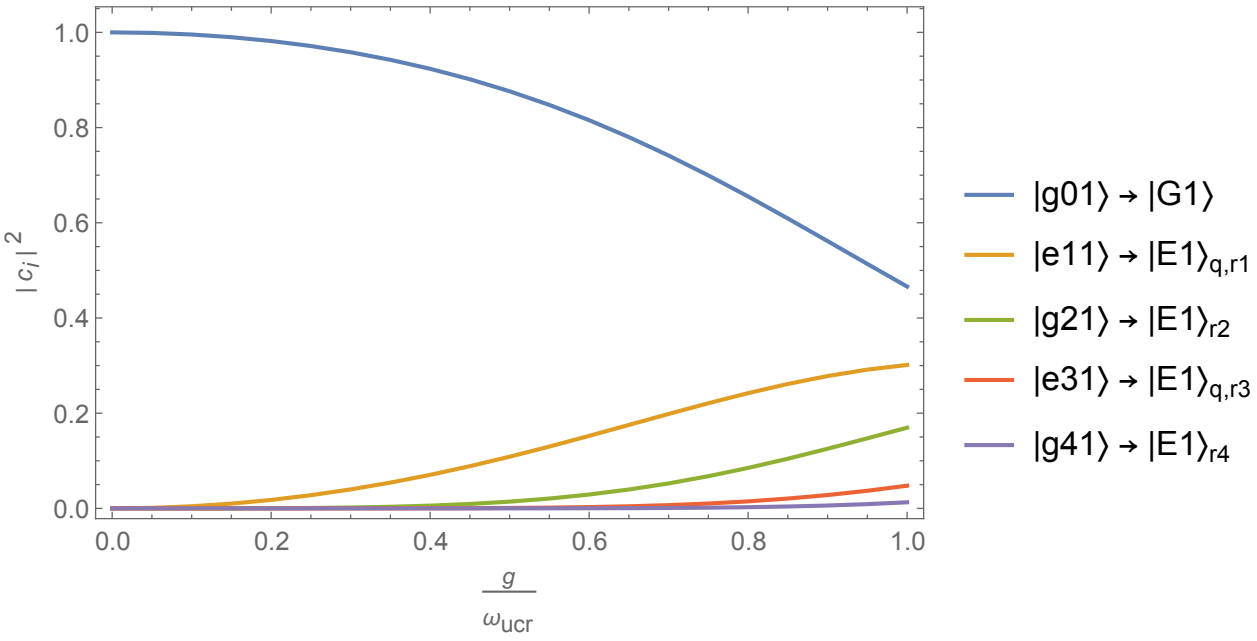

Figure : The decomposition of the state $|G1\rangle$ to the other states with respect to g coupling.

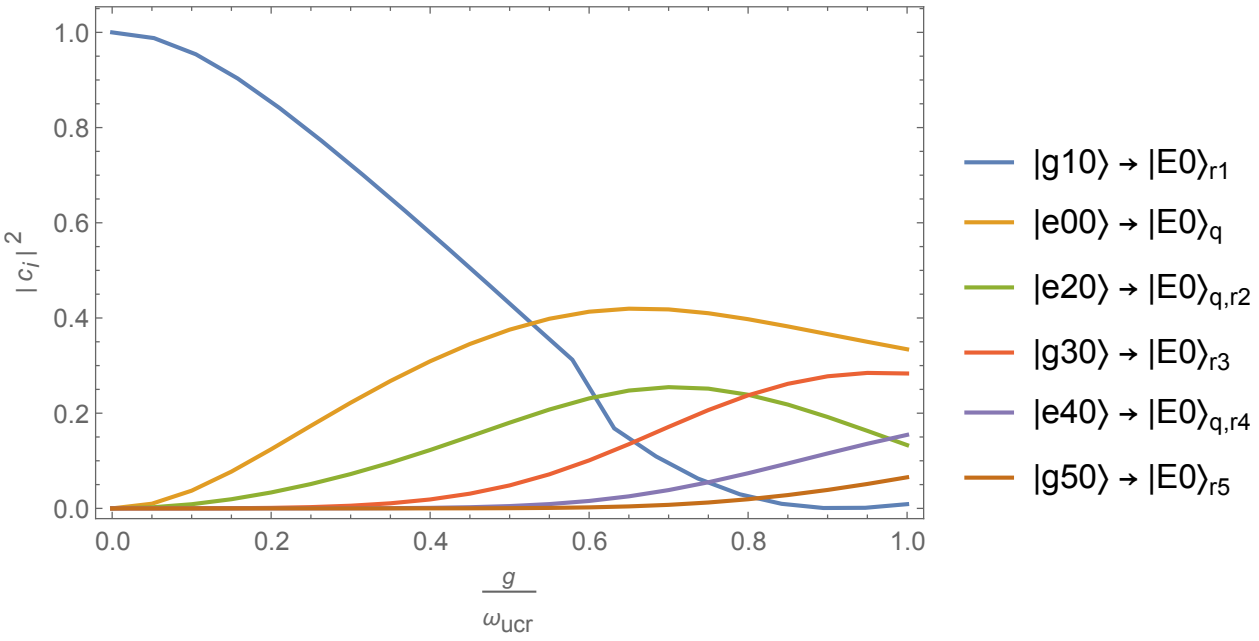

Figure : The decomposition of the state $|E0\rangle_{r1}$ to the other states with respect to g coupling.

$$
\begin{array}{ccccccc}
|g00\rangle & \leftrightarrow & |e10\rangle & \leftrightarrow & |g20\rangle & \leftrightarrow & \dots \\
 & & \updownarrow & & \updownarrow & & \\
 & & |e01\rangle & & |g11\rangle & & \\
 & & & & \updownarrow & & \\
 & & & & |g02\rangle & &
\end{array}
$$

$$
\begin{array}{ccccccc}
|e00\rangle & \leftrightarrow & |g10\rangle & \leftrightarrow & |e20\rangle & \leftrightarrow & \dots \\
 & & \updownarrow & & \updownarrow & & \\
 & & |g01\rangle & & |e11\rangle & & \\
 & & & & \updownarrow & & \\
 & & & & |e02\rangle & &
\end{array}
$$

$$
\begin{array}{ccccccc}
 & & & & |e20\rangle & |g30\rangle & \\
 & & & & \updownarrow & \updownarrow & \\
 & & |g01\rangle & \leftrightarrow & |e11\rangle & |g21\rangle & \leftrightarrow \dots \\
 & & \updownarrow & & \updownarrow & \updownarrow & \\
|e00\rangle & \leftrightarrow & |g10\rangle & & |e02\rangle & |g12\rangle & \\
 & & & & & \updownarrow & \\
 & & & & & |g03\rangle &
\end{array}
$$

$$
\begin{array}{ccccccc}
 & & & & |g10\rangle & |e30\rangle & \\
 & & & & \updownarrow & \updownarrow & \\
|e01\rangle & \leftrightarrow & & & |g11\rangle & |e21\rangle & \leftrightarrow \dots \\
 & & & & \updownarrow & \updownarrow & \\
 & & & & |g01\rangle & |e12\rangle & \\
 & & & & & \updownarrow & \\
 & & & & & |e03\rangle &
\end{array}
$$

The energy level structure:

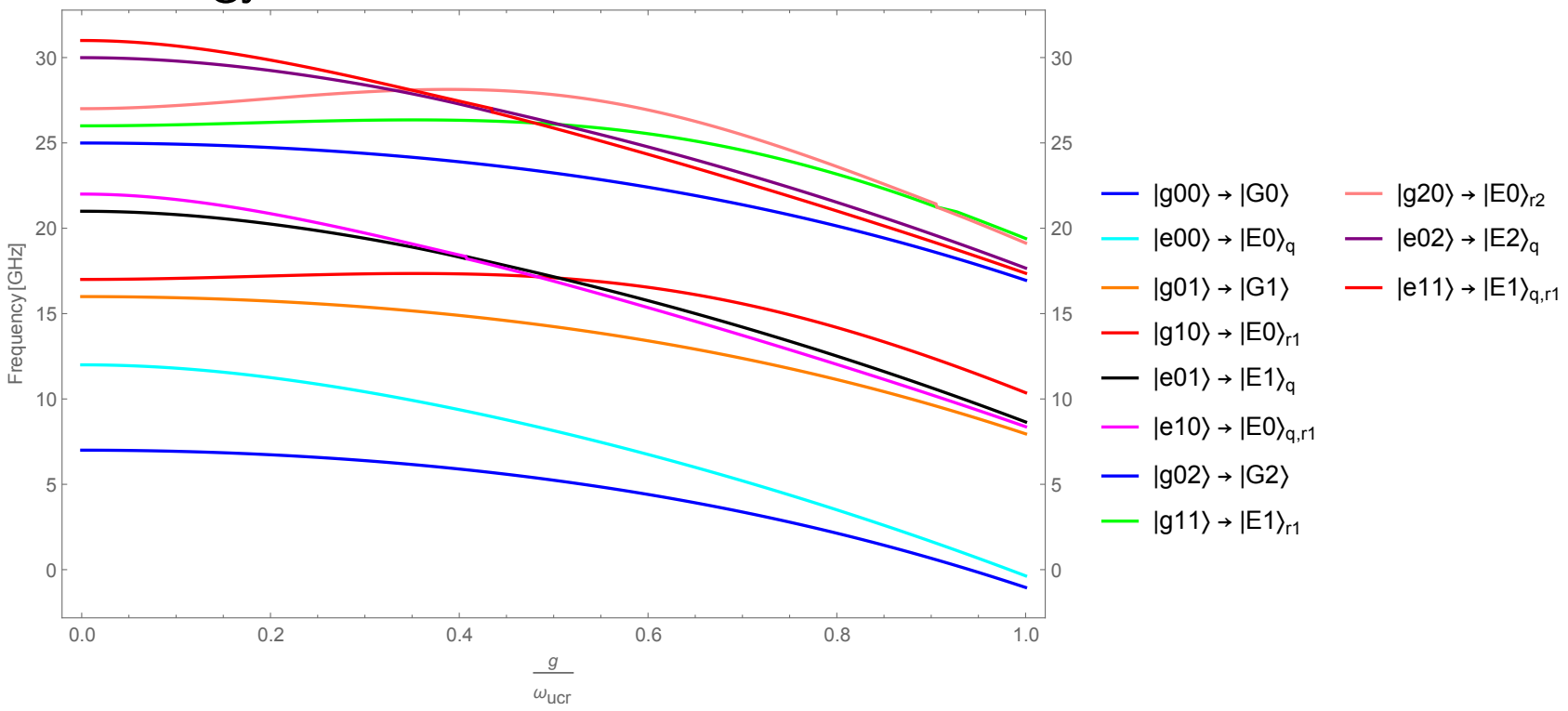

Figure : The energy levels of qubit-UCR-RR system at symmetry point, $f = 0.5$ with respect to g/ω_{UCR}.

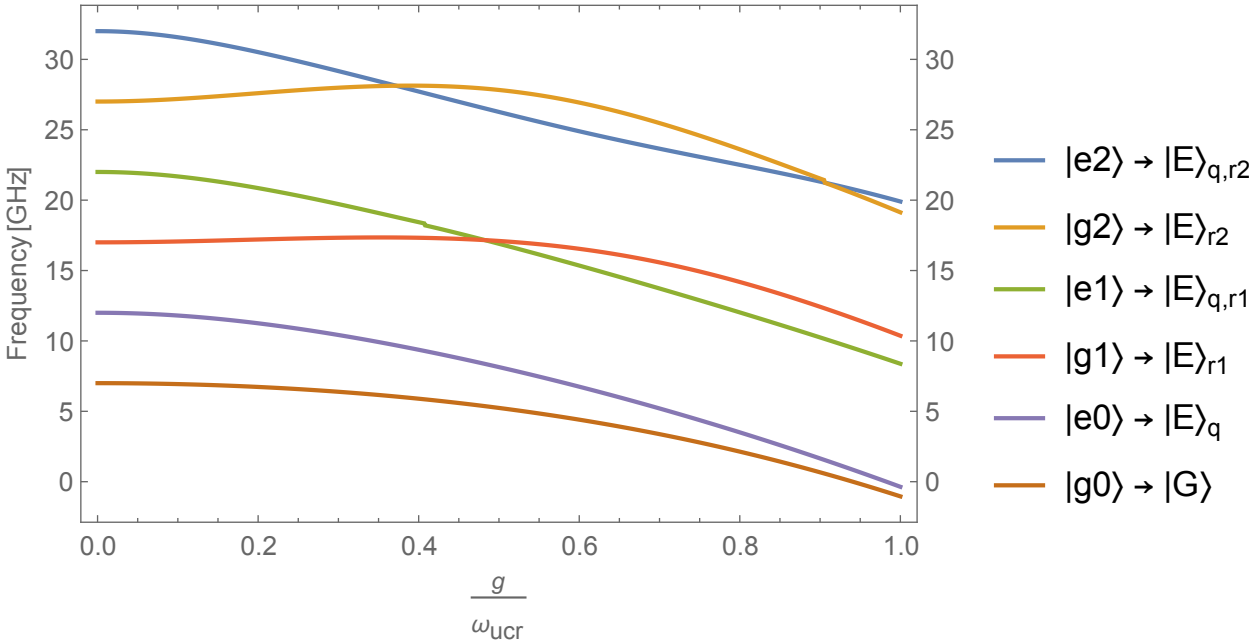

Figure : The energy levels of only qubit-UCR states of qubit-UCR-RR system at symmetry point, $f = 0.5$ with respect to g/ω_{UCR}.

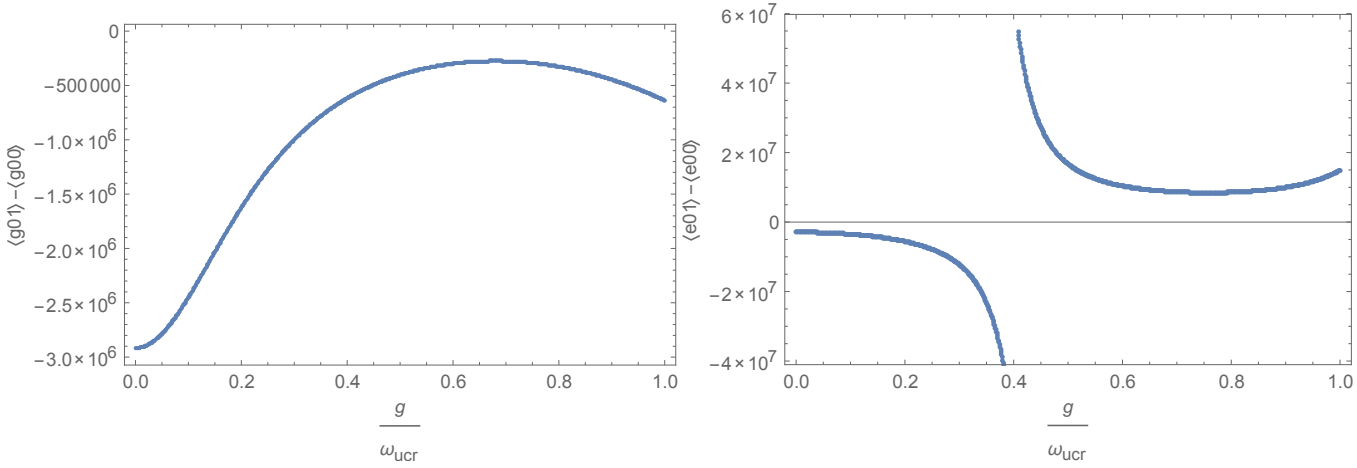

Figure : The energy shift between $\langle g01\rangle - \langle g00\rangle$ and $\langle e01\rangle - \langle e00\rangle$, respectively.

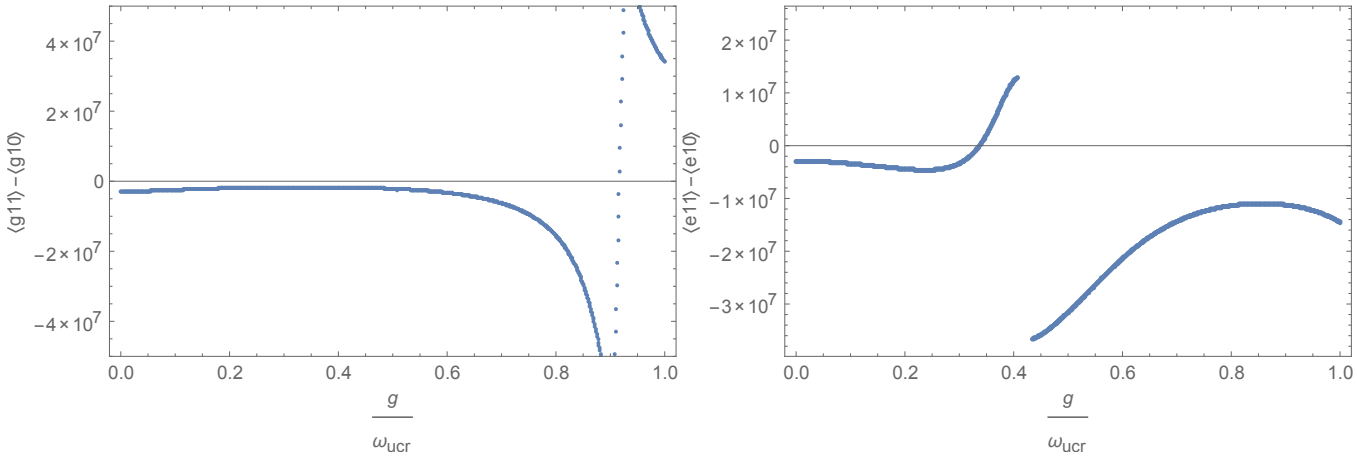

Figure : The energy shift between $\langle g11\rangle - \langle g10\rangle$ and $\langle e11\rangle - \langle e10\rangle$, respectively.

Outline

- The first and second sets of parameters are usable, though in the third set (with a detuning of 0.5 GHz) RR is quite entangled to the rest of the system.
- The numerical results point out to a possible QND measurement setup for Rabi Model in the ultrastrong coupling regime.
- An analytic expression for the energy shifts and the possibility of a readout-qubit for further research.

- PRL **107**, 100401 (2011)
- PRL **105**, 263603 (2010)
- Science, **285**, 1036 (1999)
- PRL A, **81**, 042311 (2010)